

Supplementary Material for “Hindsight is 2020 vision: Characterisation of the global response to the COVID-19 pandemic”

David J. Warne^{1,2}, Anthony Ebert³, Christopher Drovandi^{1,2},
Antonietta Mira^{3,4}, and Kerrie Mengersen^{1,2}

¹School of Mathematical Sciences, Queensland University of Technology,
Brisbane, Australia

²Australian Research Council Centre of Excellence for Mathematical and
Statistical Frontiers

³Institute of Computational Science, Università della Svizzera italiana,
Lugano, Switzerland

⁴Dipartimento di Scienza e Alta Tecnologia, Università dell’Insubria,
Varese, Italy

April 27, 2020

Contents

Appendix A Stochastic simulation	1
Appendix B Approximate Bayesian computation	4
Appendix C Estimation of \mathcal{R}_0 and \mathcal{R}_e	6
Appendix D Marginal posterior comparisons	7
Appendix E Alternative utility functions	16

Appendix A Stochastic simulation

We consider a stochastic epidemiological model across a country with population P that consists of the sub-populations, S (susceptible), I (undocumented infected), A (confirmed active), R (confirmed recovered), D (confirmed death), and R^u (undocumented

recovered). Individuals from these sub-populations interact according to the events

$$\begin{aligned}\mathcal{E}_1 : S + I &\xrightarrow{\alpha_0 + \frac{\alpha}{1 + U(A, R, D)^n}} 2I, \\ \mathcal{E}_2 : I &\xrightarrow{\gamma} A, \\ \mathcal{E}_3 : A &\xrightarrow{\beta} R, \\ \mathcal{E}_4 : A &\xrightarrow{\delta} D, \\ \mathcal{E}_5 : I &\xrightarrow{\eta\beta} R^u,\end{aligned}$$

where $U(A, R, D)$ is the utility function of observables, and model parameters related to the event rates are $\alpha_0 > 0$, $\alpha > 0$, $n \geq 0$, $\gamma > 0$, $\beta > 0$, $\delta > 0$, and $\eta > 0$. Let $\mathbf{X}_t = [S_t, I_t, A_t, R_t, D_t, R_t^u]^T$ be the state vector of sub-population counts at time $t > 0$, and assume a well-mixed population of size P .

Conditional on the state \mathbf{X}_t , the waiting time to the next occurrence of event \mathcal{E}_j is assumed to be exponentially distributed with rate parameter $h_j(\mathbf{X}_t)$, where $h_j(\mathbf{X}_t)$ is the hazard function for \mathcal{E}_j . The hazard functions can be interpreted as the instantaneous rate of events conditional on the current state. The hazard functions of our model are:

$$\begin{aligned}h_1(\mathbf{X}_t) &= \left(\alpha_0 + \frac{\alpha}{1 + U(A_t, R_t, D_t)^n} \right) \frac{S_t I_t}{P}, \\ h_2(\mathbf{X}_t) &= \gamma I_t, \\ h_3(\mathbf{X}_t) &= \beta A_t, \\ h_4(\mathbf{X}_t) &= \delta D_t, \\ h_5(\mathbf{X}_t) &= \eta \beta I_t.\end{aligned}$$

Should event j occur, the state vector is updated by adding the state change vector ν_j . For our model we have, $\nu_1 = [-1, 1, 0, 0, 0, 0]^T$, $\nu_2 = [0, -1, 1, 0, 0, 0]^T$, $\nu_3 = [0, 0, -1, 1, 0, 0]^T$, $\nu_4 = [0, 0, -1, 0, 1, 0]^T$, and $\nu_5 = [0, -1, 0, 0, 0, 1]^T$. The resulting stochastic process, $\{\mathbf{X}_t\}_{t \geq 0}$, is a discrete-state, continuous-time Markov process that can be described by

$$\mathbf{X}_t = \mathbf{X}_0 + \sum_{j=1}^5 Y_j(\lambda_j(t)) \nu_j,$$

where \mathbf{X}_0 is the initial state vector, ν_j is the state change that occurs under event j , and $Y_j(\lambda_j(t))$ is a non-homogeneous Poisson process for event j with time-dependent rate $\lambda_j(t) = \int_0^t h_j(\mathbf{X}_s) ds$. While exact realisations of this process can be generated using event-based simulation, this is prohibitive within an approximate Bayesian computational setting. Therefore, we apply a first order approximation to the integral over the interval $[t, t + \tau)$ to obtain the tau-leaping approximation [3],

$$\mathbf{X}_{t+\tau} = \mathbf{X}_t + \sum_{j=1}^5 Y_j(h_j(\mathbf{X}_t)\tau) \nu_j + \mathcal{O}(\tau),$$

where $Y_j(h_j(\mathbf{X}_t)\tau) \sim \text{Poisson}(h_j(\mathbf{X}_t)\tau)$ counts the number of times event j occurs in the interval $[t, t + \tau)$. For our simulations we use $\tau = 1/2$ (days), and initial condition

$\mathbf{X}_0 = [P - \kappa A_0 - (A_0 + R_0 + D_0), \kappa A_0, A_0, R_0, D_0, 0]$, where A_0, R_0 and D_0 come from the Johns Hopkins University COVID-19 data.

The novelty of our model is the inclusion of the utility function in the transmission process. This enable complex nonlinear dynamics arising form continuous changes in community responses over time, without explicit modelling of specific intervention dynamics. As a result, we are able to analyse the overall effect of interventions and community responses across diverse regions.

Appendix B Approximate Bayesian computation

We apply Bayesian inference to quantify uncertainty in the model parameters $\theta = [\alpha_0, \alpha, \beta, \gamma, \delta, \eta, n, \kappa]$ for country i using Johns Hopkins University data \mathcal{D}_i . Again, we omit the country index i for notational convenience. Since the full model state vector is only partially observable, the exact likelihood is intractable. We apply approximate Bayesian computation (ABC), that samples from an approximation to the posterior for each country,

$$p(\theta | \mathcal{D}) \approx p(\theta | \rho(\mathcal{D}, \mathcal{D}_s) \leq \epsilon) \propto \mathbb{P}(\rho(\mathcal{D}, \mathcal{D}_s) \leq \epsilon | \theta)p(\theta),$$

where \mathcal{D} is the COVID-19 data for the country of interest, $\mathcal{D}_s \sim s(\cdot | \theta)$ is simulated data, $\rho(\mathcal{D}, \mathcal{D}_s)$ is a discrepancy metric, ϵ is the discrepancy threshold and $p(\theta)$ is the prior. For our implementation, we apply the discrepancy metric,

$$\rho(\mathcal{D}, \mathcal{D}_s) = \left(\sum_{t=1}^{T_d} (A_t - A_{t,s})^2 + (R_t - R_{t,s})^2 + (D_t - D_{t,s})^2 \right)^{1/2}$$

where $\mathcal{D} = [\{A_t, R_t, D_t\}_{t \geq 0}]$ is the data and $\mathcal{D}_s = [\{A_{t,s}, R_{t,s}, D_{t,s}\}_{t \geq 0}]$ is simulated data.

We apply a sequential Monte Carlo scheme to move an initial set of N_p samples from the prior through a sequence of ABC approximations defined by a decreasing sequence of T discrepancy thresholds, $\epsilon_1 > \epsilon_2 > \dots > \epsilon_T = \epsilon$. Our particular implementation (Algorithm 1), based on the work of Drovandi and Pettit [2], adaptively selects the acceptance thresholds and utilises MCMC steps using tuned Gaussian random walk proposals for the move steps.

Algorithm 1 Adaptive SMC sampler for approximate Bayesian computation

```
1: Initialise  $N_a = aN_p$ ,  $N_\ell = N_p - N_a$ 
2: for  $j \in [1, 2, \dots, N_p]$  do
3:   Sample prior,  $\theta^* \sim p(\cdot)$  and simulate model,  $\mathcal{D}_s \sim s(\cdot | \theta^*)$ ;
4:   Set  $\rho_j \leftarrow \rho(\mathcal{D}, \mathcal{D}_s)$ ;
5: end for
6: repeat
7:   Sort particles  $\{(\theta_j, \rho_j)\}_{j=1}^{N_p}$ , such that  $\rho_j \leq \rho_{j+1}$  for all  $j \in [1, 2, \dots, N_p - 1]$ ;
8:   Remove particles  $\{(\theta_j, \rho_j)\}_{j=N_\ell+1}^{N_p}$  an set  $\epsilon \leftarrow \rho_{N_\ell}$ ;
9:   Resample particles  $\{\theta_j\}_{j=N_\ell+1}^{N_p}$  from  $\{(\theta_j)\}_{j=1}^{N_\ell}$  with replacement;
10:  Estimate  $\hat{\Sigma}$  of  $\{\theta_j\}_{j=1}^{N_p}$  and adapt proposal kernel  $q(u | v) = \phi\left(u; v, (2.38/8)\hat{\Sigma}\right)$ ;
11:  Set  $p_{\text{acc}} \leftarrow 0$ ;
12:  for  $j \in [N_\ell + 1, N_\ell + 2, \dots, N_p]$  do
13:    for  $k \in [1, 2, \dots, R_{\text{trial}}]$  do
14:      Generate proposal,  $\theta^* \sim q(\cdot | \theta_j)$  and sample  $u \sim \mathcal{U}(0, 1)$ ;
15:      if  $u \leq \min\left(1, \frac{p(\theta^*)q(\theta_j | \theta^*)}{p(\theta_j)q(\theta^* | \theta_j)}\right)$  then
16:        Simulate model  $\mathcal{D}_s \sim s(\cdot | \theta^*)$ ;
17:        if  $\rho(\mathcal{D}_i, \mathcal{D}_s) \leq \epsilon$  then
18:          Set  $\theta_j \leftarrow \theta^*$ ,  $\rho_j \leftarrow \rho(\mathcal{D}_i, \mathcal{D}_s)$ , and  $p_{\text{acc}} \leftarrow p_{\text{acc}} + (R_{\text{trial}}N_a)^{-1}$ ;
19:        end if
20:      end if
21:    end for
22:  end for
23:  Set  $R \leftarrow \log c / \log(1 - p_{\text{acc}})$ ;
24:  for  $j \in [N_\ell + 1, N_\ell + 2, \dots, N_p]$  do
25:    for  $k \in [1, 2, \dots, R - R_{\text{trial}}]$  do
26:      Generate proposal,  $\theta^* \sim q(\cdot | \theta_j)$  and sample  $u \sim \mathcal{U}(0, 1)$ ;
27:      if  $u \leq \min\left(1, \frac{p(\theta^*)q(\theta_j | \theta^*)}{p(\theta_j)q(\theta^* | \theta_j)}\right)$  then
28:        Simulate model  $\mathcal{D}_s \sim s(\cdot | \theta^*)$ ;
29:        if  $\rho(\mathcal{D}_i, \mathcal{D}_s) \leq \epsilon$  then
30:          Set  $\theta_j \leftarrow \theta^*$ ,  $\rho_j \leftarrow \rho(\mathcal{D}_i, \mathcal{D}_s)$ , and  $p_{\text{acc}} \leftarrow p_{\text{acc}} + (RN_a)^{-1}$ ;
31:        end if
32:      end if
33:    end for
34:  end for
35: until  $p_{\text{acc}} < p_{\text{min}}$ 
```

Appendix C Estimation of \mathcal{R}_0 and \mathcal{R}_e

Here, we derive the form of the basic reproductive number, \mathcal{R}_0 , for our model under the assumption of a mean-field approximation. The basic reproduction number after regulation (denoted \mathcal{R}_e), takes the same form but evaluates the utility function for observables at the end of the time series. We follow the method of Diekmann et al. [1]. That is, we linearize the infectious subsystem, compute the next generation matrix, and find the dominant eigenvalue about the fully susceptible population state.

The linearized mean-field infectious subsystem is (See Diekmann et al. [1]),

$$\begin{aligned}\frac{dI}{dt} &= \left(\alpha_0 + \frac{\alpha}{1+u^n}\right)I - (\gamma + \eta\beta)I, \\ \frac{dA}{dt} &= \gamma I - (\beta + \delta)A,\end{aligned}$$

where u is a prescribed constant representing regulatory strength. For computing \mathcal{R}_0 , $u = 0$ whereas for \mathcal{R}_e we set $u = C_T$. The Jacobian matrix is decomposed into the transmission matrix,

$$\mathbf{T} = \begin{bmatrix} \alpha_0 + \frac{\alpha}{1+u^n} & 0 \\ 0 & 0 \end{bmatrix}$$

and the transition matrix

$$\mathbf{\Sigma} = \begin{bmatrix} -(\gamma + \eta\beta) & 0 \\ \gamma & -(\beta + \delta) \end{bmatrix}.$$

The next generation matrix is prescribed by $\mathbf{K} = -\mathbf{T}\mathbf{\Sigma}^{-1}$, that is,

$$\mathbf{K} = - \begin{bmatrix} \alpha_0 + \frac{\alpha}{1+u^n} & 0 \\ 0 & 0 \end{bmatrix} \begin{bmatrix} -\frac{1}{\gamma + \eta\beta} & 0 \\ -\frac{\gamma}{(\gamma + \eta\beta)(\beta + \delta)} & -\frac{1}{\beta + \delta} \end{bmatrix} = \begin{bmatrix} \alpha_0 + \frac{\alpha}{1+u^n} & 0 \\ \frac{\gamma}{\gamma + \eta\beta} & 0 \end{bmatrix}.$$

Since $\det(\mathbf{K}) = 0$ we have $\mathcal{R}_0 = \text{trace}(\mathbf{K})$. Therefore, $\mathcal{R}_0 = \frac{\alpha_0 + \alpha}{\gamma + \eta\beta}$, and $\mathcal{R}_e = \frac{\alpha_0 + \frac{\alpha}{1+C_T^n}}{\gamma + \eta\beta}$ where C_T is the cumulative number of confirmed cases at the end of the data time series.

Appendix D Marginal posterior comparisons

This section includes box-plots for comparison of posterior distributions across countries for each model parameter for the two time periods 22 January–31 March 2020 (Fig. 1–4) and 22 January–13 April 2020 (Fig. 5–8). For reference, Table 1 provides the ISO-3166 alpha3 codes for each country.

Table 1: Lookup table of Country names by ISO-3166 alpha3 codes

Country Code	Country Name	Country Code	Country Name
AFG	Afghanistan	JPN	Japan
ALB	Albania	KAZ	Kazakhstan
AND	Andorra	KHM	Cambodia
ARE	United Arab Emirates	KOR	South Korea
ARG	Argentina	KWT	Kuwait
ARM	Armenia	LBN	Lebanon
AUS	Australia	LKA	Sri Lanka
AUT	Austria	LTU	Lithuania
AZE	Azerbaijan	LUX	Luxembourg
BEL	Belgium	LVA	Latvia
BFA	Burkina Faso	MAR	Morocco
BGR	Bangladesh	MDA	Moldova
BHR	Bahrain	MEX	Mexico
BIH	Bosnia and Herzegovina	MKD	North Macedonia
BRA	Brazil	MLT	Malta
BRN	Brunei	MUS	Mauritius
CAN	Canada	MYS	Malaysia
CHE	Switzerland	NGA	Nigeria
CHL	Chile	NLD	Netherlands
CHN	China	NOR	Norway
CIV	Cote d'Ivoire	NZL	New Zealand
CMR	Cameroon	OMN	Oman
COL	Columbia	PAK	Pakistan
CRI	Costa Rica	PAN	Panama
CUB	Cuba	PER	Peru
CYP	Cyprus	PHL	Philippines
CZE	Czechia	POL	Poland
DEU	Germany	PRT	Portugal
DNK	Denmark	PSE	Palestine
DOM	Dominican Republic	QAT	Qatar
DZA	Algeria	ROU	Romania
ECU	Ecuador	RUS	Russia
EGY	Egypt	SAU	Saudi Arabia
ESP	Spain	SEN	Senegal
EST	Estonia	SGP	Singapore
FIN	Finland	SMR	San Marino
FRA	France	SRB	Serbia
GBR	United Kingdom	SVK	Slovakia
GHA	Ghana	SVN	Slovenia
GRC	Greece	SWE	Sweden
HND	Honduras	THA	Thailand
HRV	Croatia	TUN	Tunisia
HUN	Hungary	TUR	Turkey
IDN	Indonesia	TWN	Taiwan
IND	India	UKR	Ukraine
IRL	Republic of Ireland	URY	Uruguay
IRN	Iran	USA	United States
IRQ	Iraq	UZB	Uzbekistan
ISL	Iceland	VEN	Venezuela
ISR	Israel	VNM	Vietnam
ITA	Italy	ZAF	South Africa
JOR	Jordan		

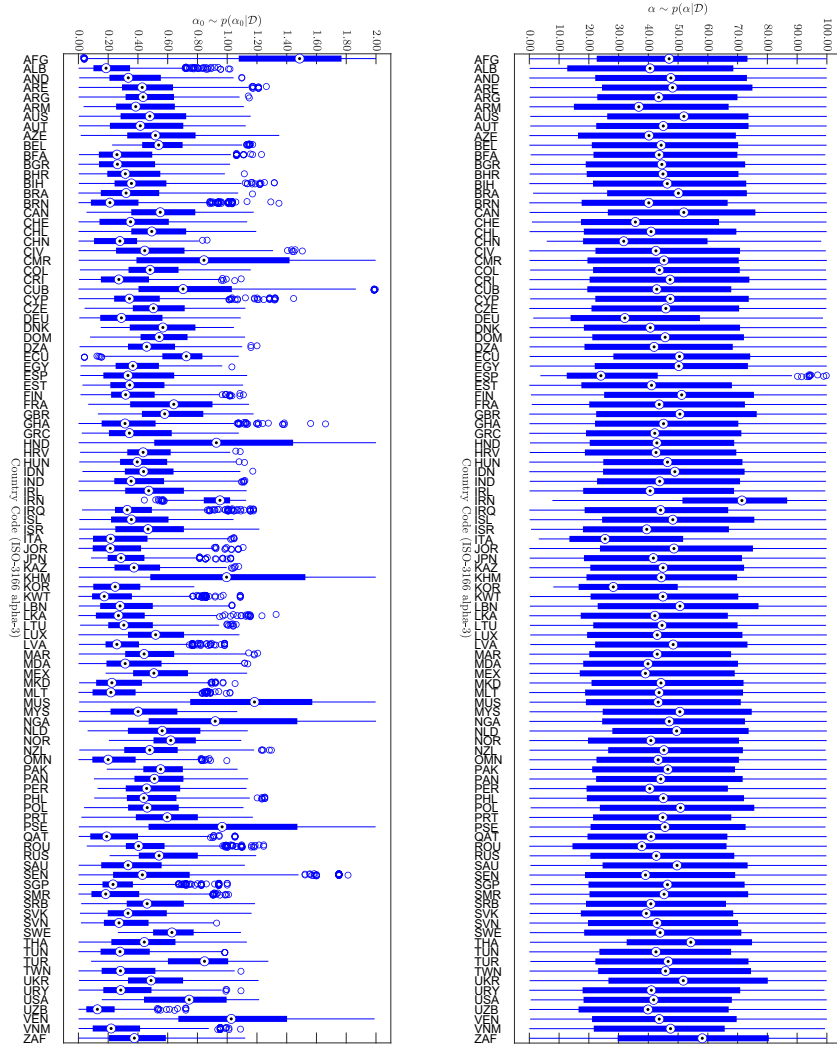


Figure 1: Box plots comparing marginal posterior distributions by country over the period 22 January–31 March 2020 for transmission rate parameters α_0 (left) and α (right).

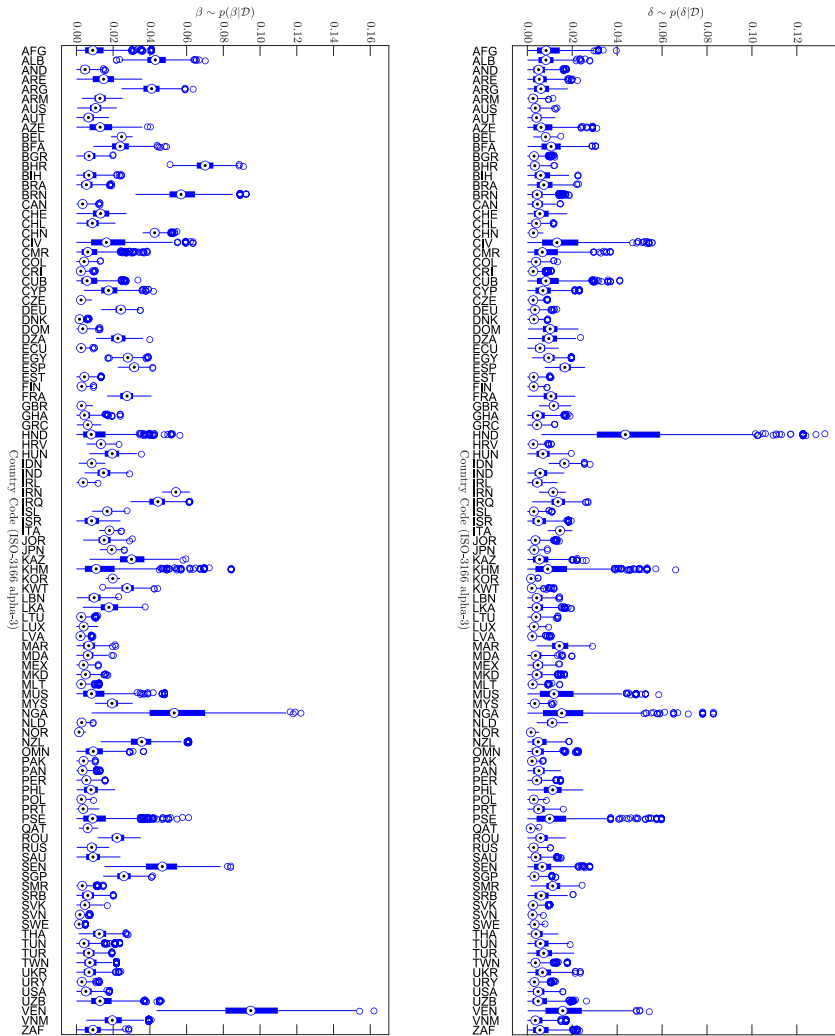


Figure 2: Box plots comparing marginal posterior distributions by country over the period 22 January–31 March 2020 for case recovery rate parameter β (left) and case death rate δ (right).

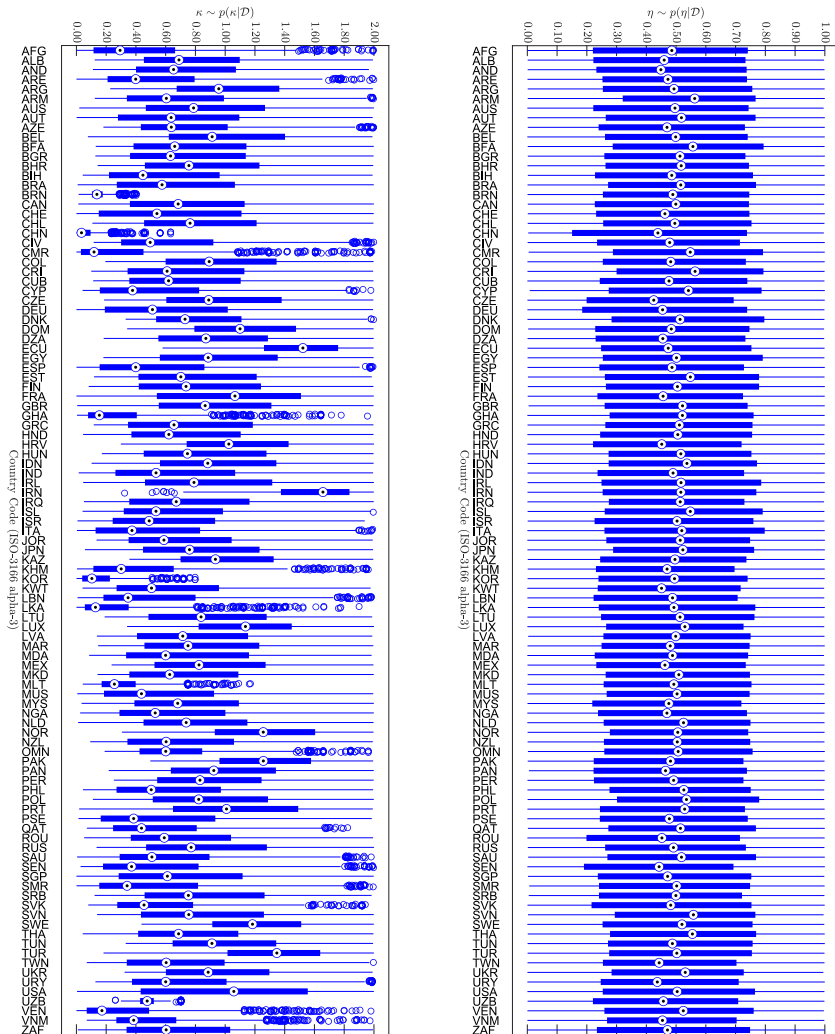


Figure 3: Box plots comparing marginal posterior distributions by country over the period 22 January–31 March 2020 for initial infected scale parameter κ (left) and relative recovery rate η (right).

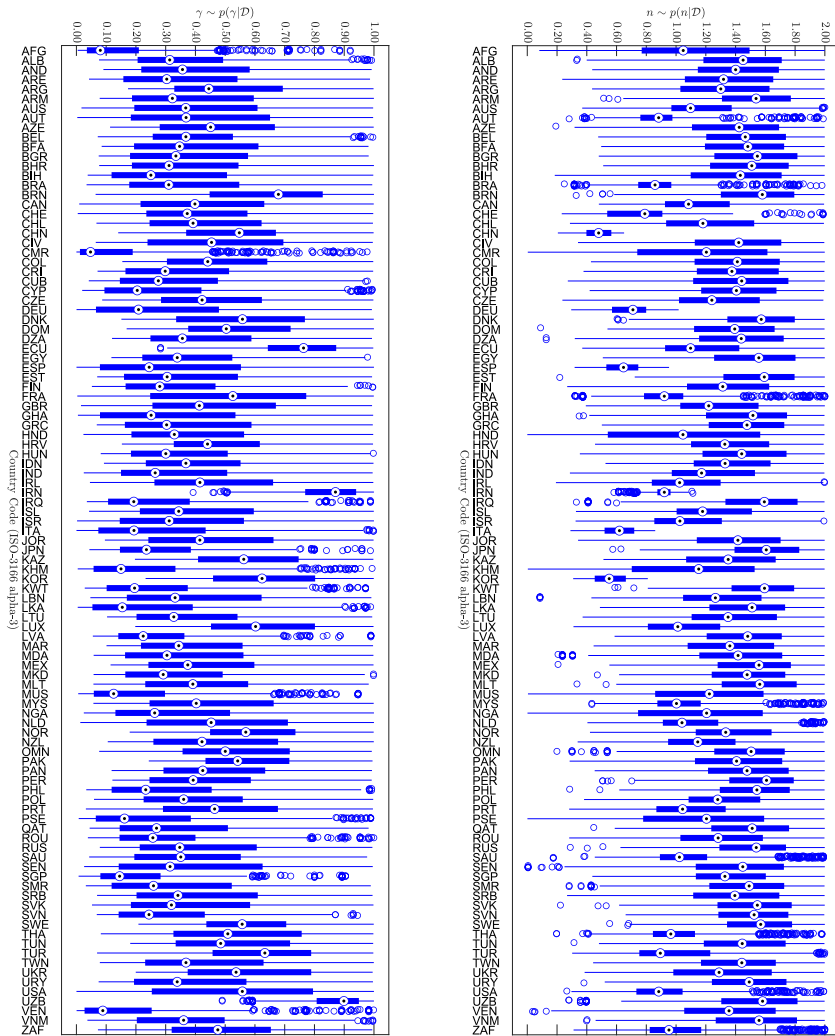


Figure 4: Box plots comparing marginal posterior distributions by country over the period 22 January–31 March 2020 for identification rate γ (left) and regulatory parameter n (right).

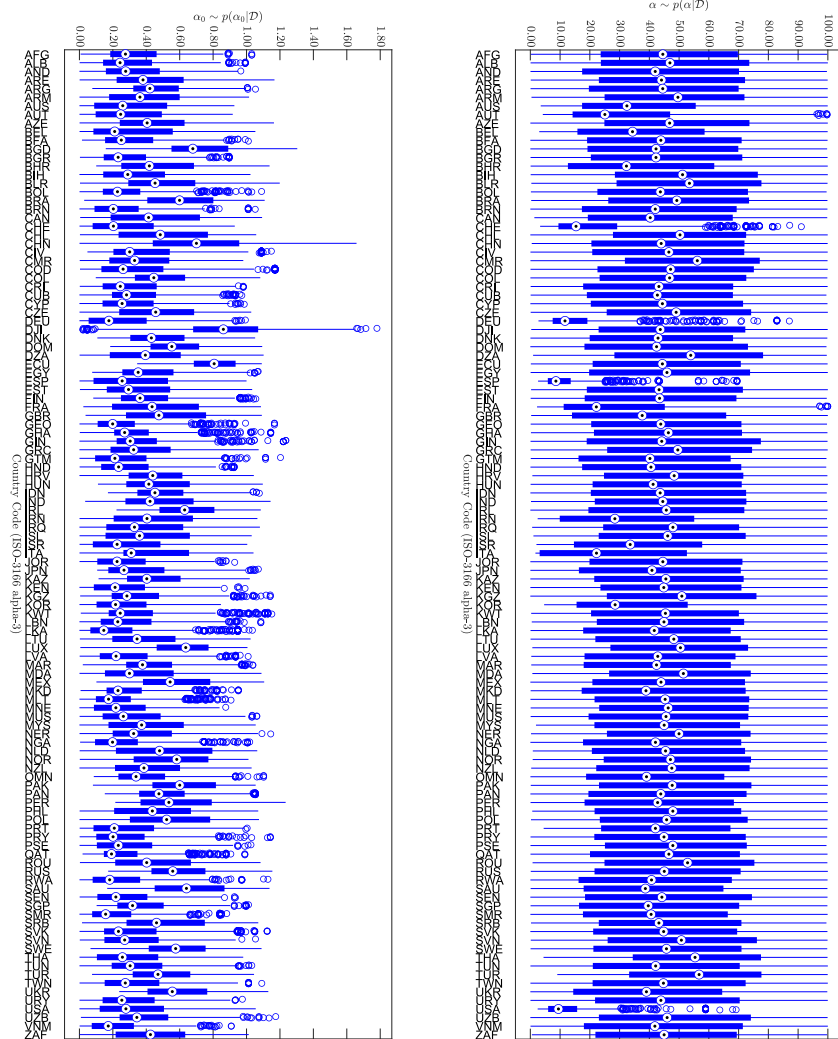


Figure 5: Box plots comparing marginal posterior distributions by country over the period 22 January–13 April 2020 for transmission rate parameters α_0 (left) and α (right).

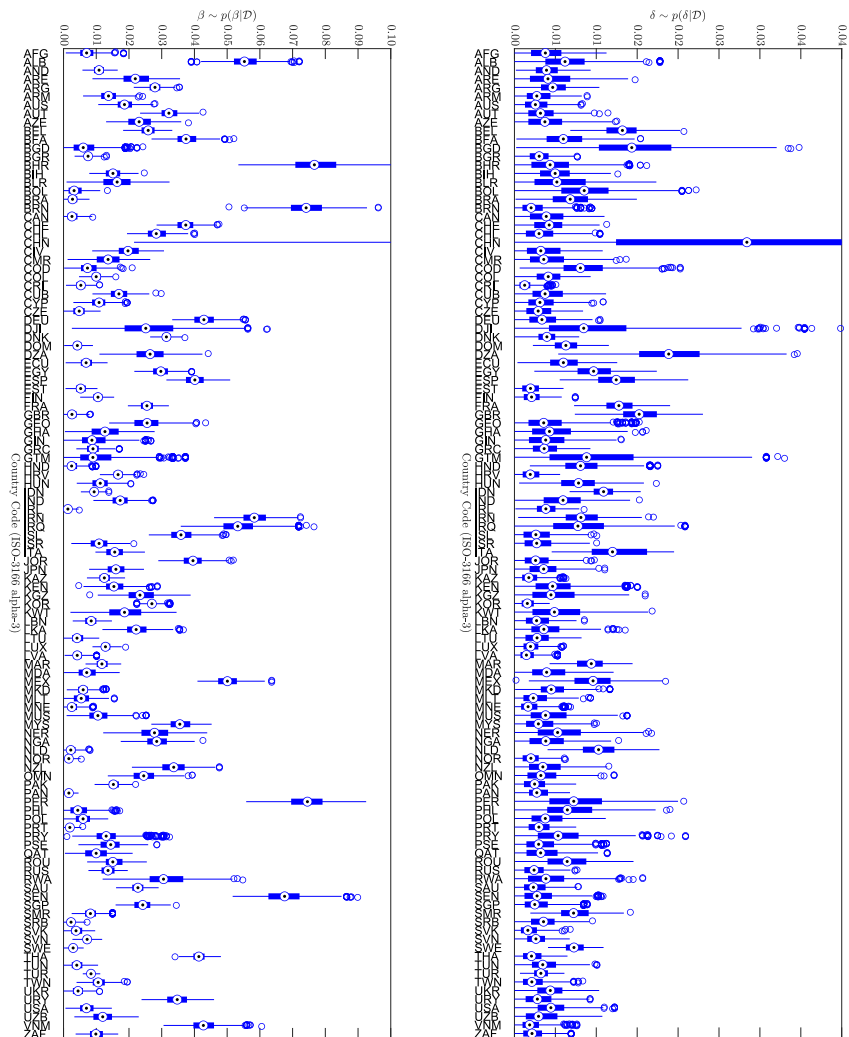


Figure 6: Box plots comparing marginal posterior distributions by country over the period 22 January–13 April 2020 for case recovery rate parameter β (left) and case death rate δ (right).

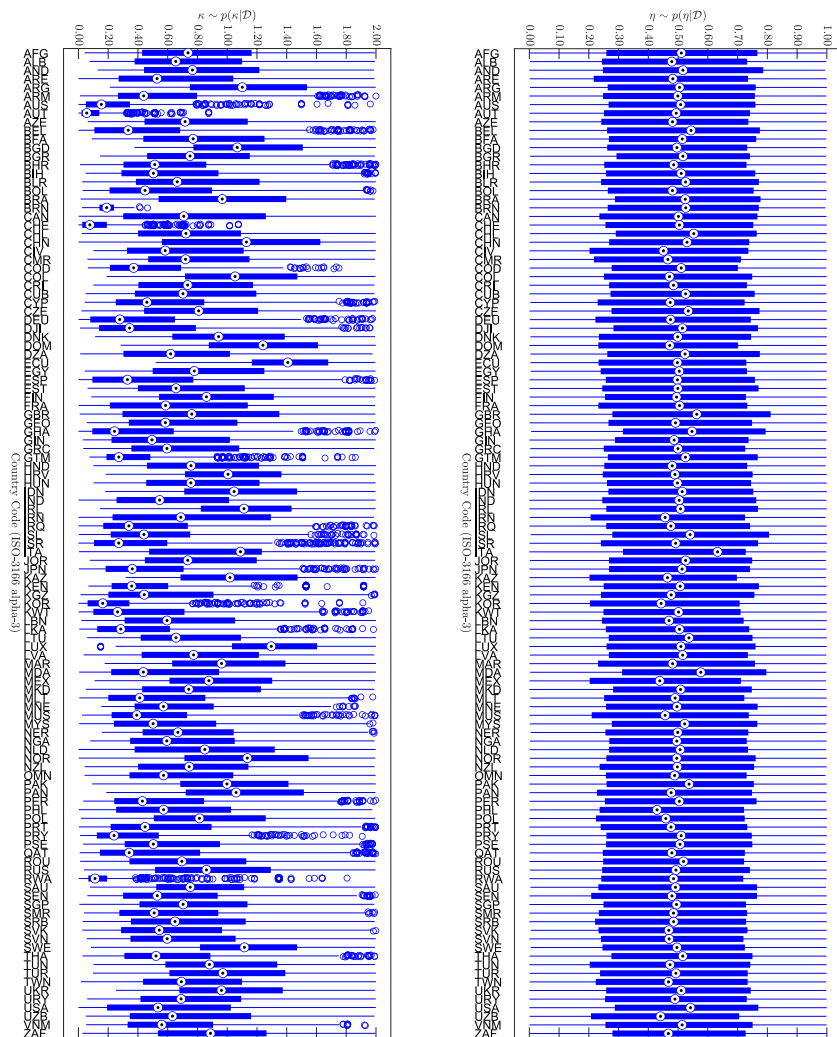


Figure 7: Box plots comparing marginal posterior distributions by country over the period 22 January–13 April 2020 for initial infected scale parameter κ (left) and relative recovery rate η (right).

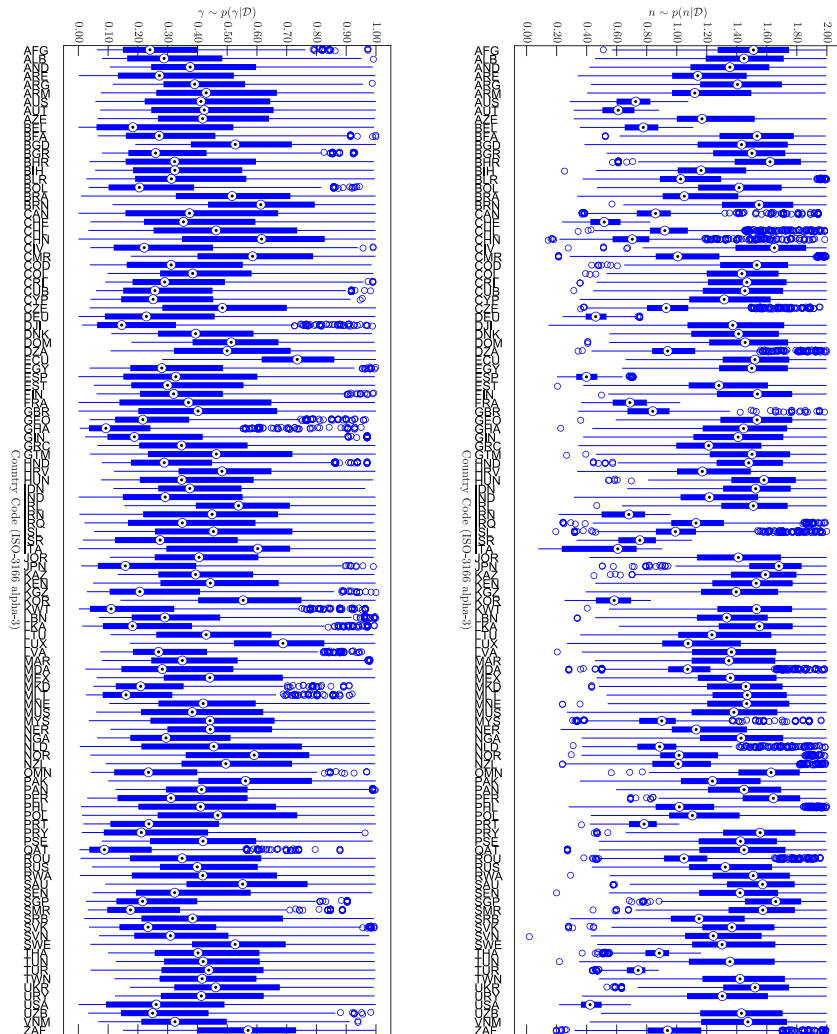


Figure 8: Box plots comparing marginal posterior distributions by country over the period 22 January–13 April 2020 for identification rate γ (left) and regulatory parameter n (right).

Appendix E Alternative utility functions

The results within the main text are based on the utility function $U(A_t, R_t, D_t) = A_t + R_t + D_t$. That is transmission rate regulation is dependent on cumulative confirmed case counts only. Other utility functions could be considered in a straightforward manner. For illustration, we considered the possibility of a community being significantly more sensitive to death counts by using the utility function $U(A_t, R_t, D_t) = D_t$. Point estimates of regulatory parameters are provided in Fig. 9. It can be seen that under this scenario the posterior predictive fitness was poor for many countries (See examples in Fig. 10). We conclude that utility based on confirmed cases is more realistic, however, more general forms could be considered by introducing region specific weighting parameters.

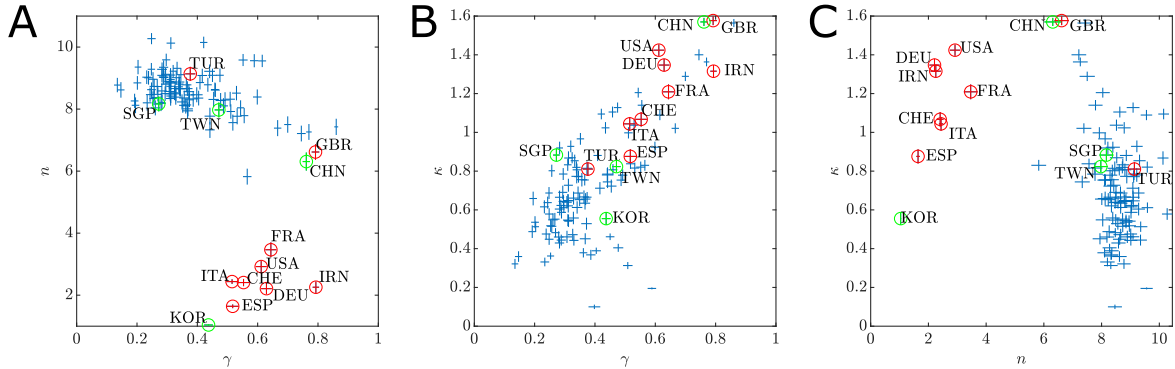


Figure 9: Pairwise scatter plots of point estimates of each assessed country (blue points, with lines to indicate 95% CI) for the key parameters related to the management of an COVID-19 outbreak up to 13 April 2020 using the death only utility function: regulatory parameter n ; detection rate γ ; and the relative initial undocumented cases κ . (A) n versus γ ; (B) κ versus γ ; and (C) κ versus n . The top ten countries for confirmed case counts are highlighted (red) along with countries that have managed to control the outbreak are highlighted (green). Labels identify the country by ISO-3166 alpha-3 code.

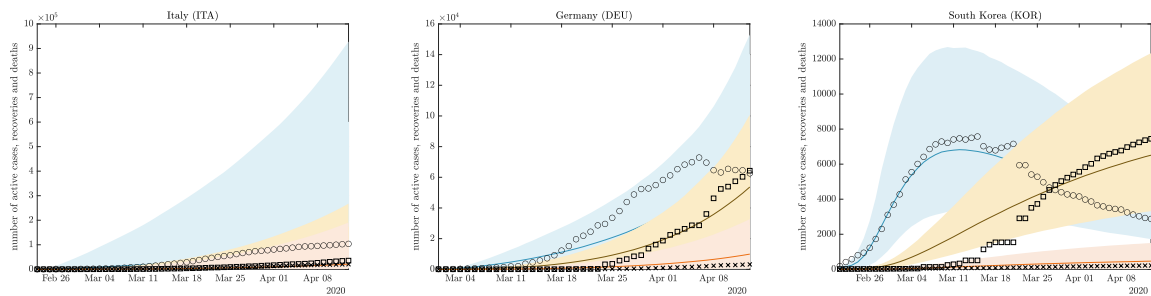


Figure 10: Examples of poor fits typical of the model when using the death only utility function. We conclude that the cumulative case utility function is a more appropriate specification for the global response pattern.

References

- [1] O. Diekmann, J. A. P. Heesterbeek, and M. G. Roberts. The construction of next-generation matrices for compartmental epidemic models. *Journal of The Royal Society*

Interface, 7(47):873–885, 2009.

- [2] C. C. Drovandi and A. N. Pettitt. Estimation of parameters for macroparasite population evolution using approximate Bayesian computation. *Biometrics*, 67(1):225–233, 2011.
- [3] D. T. Gillespie. Approximate accelerated stochastic simulation of chemically reacting systems. *The Journal of Chemical Physics*, 115(4):1716–1733, 2001.